The Fourth IEEE RAS/EMBS International Conference
on Biomedical Robotics and Biomechatronics
Roma, Italy. June 24-27, 2012

Development and Initial Testing of a General–Purpose, MR–Compatible, Manually–Actuated Manipulator for Image–Guided Interventions

Eftychios G. Christoforou, Ioannis Seimenis, Eleni Andreou, Nikolaos V. Tsekos

Abstract— **A novel MR–compatible manually–actuated robotic manipulation device has been developed. It is a general–purpose system that provides access to the patient inside a closed–cylindrical MRI scanner. It allows the performance of various minimally–invasive interventions, such as biopsies and local drug deliveries, using real–time images for guidance and monitoring. The design of the system is described and the prototype constructed is presented together with initial MRI phantom testing on needle targeting. The characteristics and potential of manual actuation in MR–compatible robotic systems are examined.**

I. INTRODUCTION

Image–guided interventions have been a most important development in interventional medicine. By exploiting radiological images various diagnostic and therapeutic interventions are currently performed more effectively in a minimally–invasive fashion using image guidance. Image–guided interventions include biopsies [1], local drug deliveries [2], aspirations, implantation of radioactive brachytherapy seeds [3], ablations (e.g., thermal ablation, cryoablation) [4], etc. Various imaging modalities are currently used for such interventions including X–rays, computed tomography (CT) and ultrasound. Magnetic resonance imaging (MRI) is also being used for interventional purposes but to a relatively lesser extent. Despite its favorable imaging capabilities two major reasons have prevented its widespread use. First, the existence of strong permanent and rapidly switching magnetic fields, needed for the MR image generation, imposes strict limitations on the type of interventional tools to be used, which in general have to be non–magnetic and non–conductive. Second, the free space inside the MR scanner is limited, thus complicating patient accessibility. Consequently, most of the MR–guided procedures are currently carried out inside open–type scanners (e.g., C–type or double–donut) which allow sufficient access to the patient. These scanners operate at relatively low magnetic fields (0.1-1 Tesla) easing restrictions on used instruments at the cost, however, of magnetic field homogeneity and quality of acquired imaging information in general. Various MR–guided interventions are also carried out stereotactically based on preoperative images as for example in various neurosurgical procedures. In general, stereotactic approaches are prone to errors due to potentially inaccurate registration, blindness to needle deflections, not consideration of tissue displacements and deformations during needle penetration, positioning errors on behalf of the tool positioning devices and inadequate patient immobilization.

Performing interventions using intraprocedural MR information is a highly advantageous option and the involvement of robotic assistance has been proposed for providing the required access to the patient inside cylindrical, closed–type scanners [5]. Such scanners have high static magnetic fields (1.5 and 3.0 Tesla) resulting in superior imaging capabilities, compared to the open–type imagers, and are widely available. The development of appropriate robotic systems entails numerous engineering challenges originating from the limited space inside the scanner as well as the magnetic nature of the modality. Similar to any object exposed to the MR environment, robotic systems are required to be MR–compatible, i.e., they have to be safe for the patient and other individuals and also not to significantly alter the quality of the imaging information [6]. Various robotic systems have been developed for realizing the necessary access to the patient, e.g., [7], [8], [9], [10].

The present work describes the prototype design and development of a novel general–purpose MR–compatible manipulation system. The system is manually actuated and provides the required access to the patient inside a closed–type cylindrical MR scanner in order to perform an intervention under real–time imaging. The characteristics and potential of manual actuation are examined within a general MR–compatible robotics framework.

II. SYSTEM DESIGN

The system was designed to provide access to the patient with the end–effector positioned near the isocenter inside the bore of a closed–type, cylindrical MR scanner. However, given the higher magnetic fields involved the MR–compatibility requirements become more stringent when compared to open scanners. A discussion regarding the existing MR scanner types and their suitability for image–guided interventions is provided in [11].

This work was supported by the European Regional Development Fund and the Republic of Cyprus through the Research Promotion Foundation (grant TEXNOLOGIA/MHX/0308(BIE)/05). NVT acknowledges partial support by the National Science Foundation (NSF) award CNS-0932272.

E.G. Christoforou is with KIOS Research Center, University of Cyprus, 75 Kallipoleos Avenue, 1687 Nicosia, Cyprus e.christoforou@ucy.ac.cy (Address for Correspondence)

I. Seimenis is with the Lab. of Medical Physics, Dept. of Medicine, Democritus University of Thrace, Alexandroupolis, Greece iseimen@med.duth.gr

E. Andreou is with the Dept. of Mechanical and Manufacturing Engineering, University of Cyprus, Cyprus andreou.d.eleni@ucy.ac.cy

N.V. Tsekos is with the Medical Robotics Lab., Dept. of Computer Science, University of Houston, Houston, TX, USA ntsekos@cs.uh.edu

978-1-4577-1198-5/12/$26.00 ©2012 IEEE

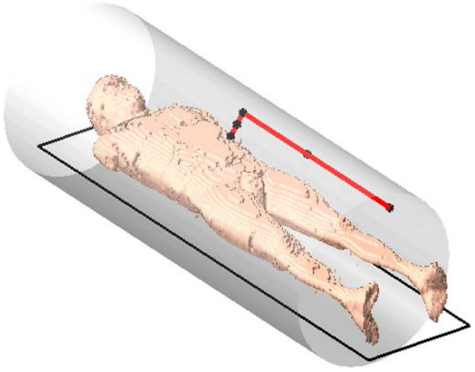

Fig. 1. Simulation tool employed as part of the design process for an initial selection of the kinematic structure as well as the dimensions of the robotic manipulation system. A digital model of a human subject is shown inside the scanner gantry together with a line representation of the arm at a selected input position.

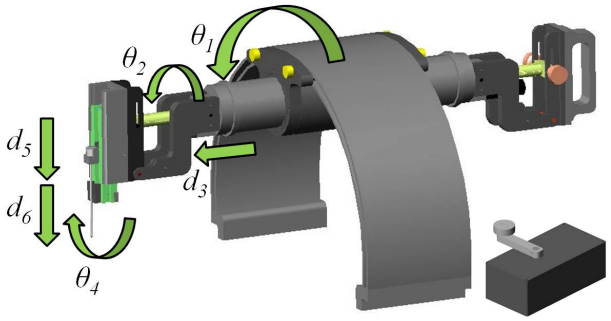

Fig. 2. A CAD model of the manipulation system depicting the available motions. The corresponding joint variables are represented as θ_i for the rotational joints and d_i for the translational ones. In the lower right corner is shown the manual hand–held needle actuation unit.

A. MR-Compatibility Design Requirements

In general, MR–compatibility of an interventional robotic system refers to each individual component of the system: materials, actuation, sensing. With a manually–actuated system, as the one considered here, there is no need for specialized actuators or sensors to provide feedback control information [12]. Therefore, the design attention focuses on the selection of suitable materials which in general are required to be nonmagnetic and nonconductive (e.g., plastic, fiberglass, wood, ceramics). Ferromagnetic materials are subject to strong magnetic forces as well as torques attempting to orient the object inside the field. This may result to static deflections (e.g., bending of a needle) or convert an object into a potentially hazardous projectile. Moreover, ferromagnetic materials create susceptibility artifacts which downgrade image quality. Conductive materials are also inappropriate for MR–compatible systems because when exposed to the scanner's switching magnetic field gradients and RF pulses eddy currents may be generated. Induced currents locally alter the homogeneity of the main magnetic field resulting to severe image artifacts. Moreover, induced currents may produce unwanted heating.

Apart from the design limitations originating from the magnetic nature of the scanning environment, "geometric MR compatibility" dictates that robotic systems are compact in shape, yet sufficiently dexterous and structurally stiff in order to meet the requirements of clinical applications. The strict space limitations related to the scanner geometry need to be taken into account and as part of the system design extensive space analyses were carried out. For this purpose volunteer images were systematically processed in order to quantify the available space inside the scanner [13]. For the initial selection of an appropriate kinematic structure and the dimensions of the manipulation system (e.g., end–effector height) simulation studies were performed. For this purpose digital models of human subjects were constructed and combined with representations of the arm, which can be manipulated inside the scanner gantry. The arm's position is calculated by the forward kinematics solution and the graphics representation is updated for the current input set of joint variables. One example is shown in Figure 1.

B. Kinematics and Physical Structure

The system developed consists of an arc–shaped supporting structure onto which the arm is attached. The main arm component extends inside the gantry to reach the patient. On one side of the arm is the control handle and at the opposite side is the application–specific end–effector. A solid model representing the design is shown in Figure 2, also depicting the available motions. The system is endowed with a totality of five degrees–of–freedom, which in general they suffice for the positioning of an axisymmetric tool (e.g., a biopsy needle) at an arbitrary position and orientation within the manipulator's workspace. The corresponding joint variables are represented as θ_i for the rotational joints (rotation angles) and as d_i for the translational joints (linear displacements). Using rotation θ_1 the overall positioning of the arm is adjusted on the arch providing a periphery access to the patient. Rotations θ_2 and θ_4 are used for adjusting the orientation of the end–effector. Linear displacement d_3 is used for the end–effector position adjustment along the length of the gantry and the displacement d_5 corresponds to a telescopic motion for nearing the patient's body surface prior to the commencement of a needle insertion. The needle insertion/removal is an additional independently controlled motion (d_6) associated with the end–effector.

The link lengths and the maximum travel for each individual joint define the extents of the manipulator's workspace and were selected based on the requirements for patient accessibility. The overall length of the arm in particular was selected so that the end–effector can operate at the vicinity of the scanner's isocenter. In that area the main magnetic field is more homogeneous and imaged anatomy distortions are avoided. Also, in that area the scanner's effective field–of–view assumes its largest size [13].

The arc–shaped base structure on which the system is mounted is an inherently strong and sufficiently rigid structural element. This specific element has also been used

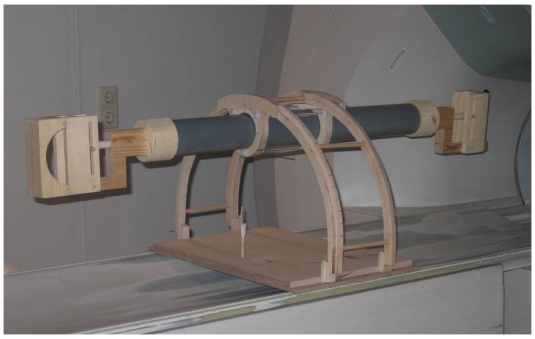

Fig. 3. As part of the design process a limited–functionality mockup of the system was constructed prior to building the actual prototype system. The mockup helped evaluate the design.

with the commercial MR–compatible system Innomotion [8], [14] where a robotic arm can be attached to an arch base at a number of distinct locations. In the current design, however, the arch not only serves as a mounting structure but also hosts a bearing along which the rest of the arm can slide and is related to one of the available motions (corresponding to θ_1 in Figure 2). The arm's position on the arch can be locked using a brakes system. Another similar mounting arrangement was used with AcuBot, a robotic system suitable for CT–based procedures [15]. In that case the robotic manipulation system is attached on a bridge–like structure that mounts on the scanner's table.

Prior to building the actual prototype system and as an intermediate step between solid modeling and prototype realization a limited–functionality MR–compatible mockup of the system was constructed, as shown in Figure 3. Wood and plastic materials were used for its construction. Its value has been indispensable in verifying the adequacy of the kinematics structure and the dimensions of the manipulation system with regard to the required patient accessibility and the "geometric MR–compatibility" of the device [13]. Following the assessment of the mockup system some dimensional adjustments were decided and the design was finalized.

C. End–Effector

The distal end of the manipulator's arm features an attachment plate onto which interchangeable end–effectors can be installed. For the purposes of this study, an end–effector suitable for needle targeting applications was constructed and attached to the tip of the arm. It can hold a general–purpose needle (e.g., for the injection of drugs or fine needle aspiration biopsies). The needle grip is attached to a slider block which moves along a guide on the end–effector to realize a needle insertion/removal.

Needle motion is manually controlled from outside the gantry via a hand–held actuation unit, included in Figure 2 and Figure 4a. The actuation unit is separate from the manipulator and includes a turning handle (crank) which rotates a drum inside the enclosure. Around the drum is wrapped a string, so that when the drum is rotated string is drawn in from one side of the drum and equal length of

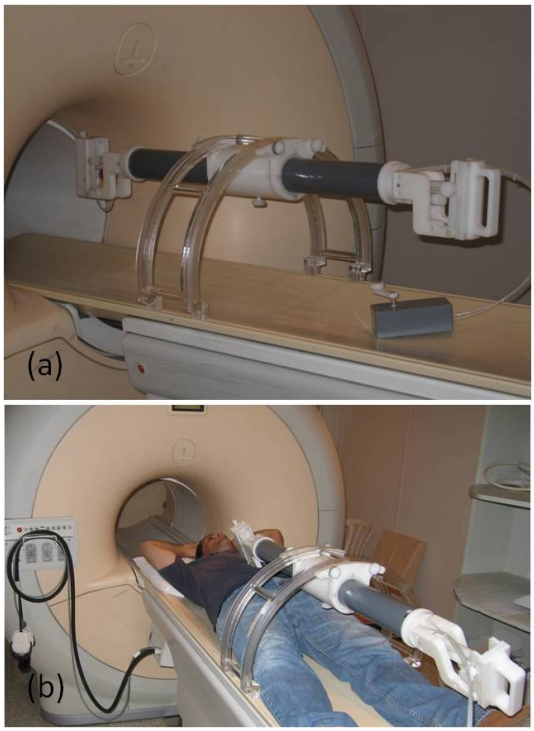

Fig. 4. (a) The prototype manipulation system installed on the MR scanner. The arm is attached to a an arch structure which directly mounts onto the patient's table. The arm is deployed inside the scanner to provide the required access to the patient. At the proximal end of the arm is the control handle and at the distal end is the end–effector. The needle insertion is controlled with a manual device shown resting on the patient's table top. (b) Demonstration of the interventional concept with a human subject accommodated on the patient's table and the manipulation system installed.

string is released from the other side. The two strings travel inside tubes to the end–effector forming a closed–loop with the needle holder (slider block). The actuation mechanism also includes a spring–loaded tension system that ensures that the strings remain stretched. The tubes inside which the strings travel are loaded in compression and are required to have adequate axial stiffness.

III. PHYSICAL PROTOTYPE

For the prototype realization a variety of plastic materials were used. The main construction material has been Polyoxymethylene (POM) which is a thermoplastic with favorable mechanical properties including high strength and stiffness, excellent dimensional stability and low friction coefficients. From a manufacturing point of view it has very good machinability. It can be shaped under conventional machining processes resulting in a good surface finish and accomplishing the required dimensional tolerances. Among the disadvantages of the specific material are the relatively high cost and the difficulty to bond using adhesives. For this reason the prototype device was assembled using plastic screws. The arch structure in specific, as well as other small–sized parts, were constructed of Plexiglas.

All individual parts of the system were produced using accurate computer numeric control (CNC) machining. The

prototype system is shown in Figure 4a mounted onto the scanner's table top. The specific mounting arrangement allows for the patient to be placed in different positions depending on the application needs: head–first, feet–first, supine, prone and also in lateral decubitus positions. The system needs to be installed after the patient is accommodated on the table as demonstrated in Figure 4b, prior to the insertion of the table in the gantry. The actual mounting option also allows for a quick removal of the system in the case of an emergency situation. The overall mass of the system is about 7 kg which allows for easy transportation and installation, which does not require a specialized technician for this purpose. The arm attached to the arch is deployed inside the scanner to reach the patient. As shown in Figure 4 and as mentioned above, at the proximal end of the arm is the control handle and the end–effector is attached at the distal end. Similar to any interventional system there will be a need for sterilization. The geometry of the system itself allows to be covered with sterile bags if required while treating any interventional tools or remaining exposed parts of the system (end–effector assembly) using appropriate sterilization agents. The fact that the system does not have any build–in sensors or actuators is also advantageous in that respect.

The particular end–effector that was used for our experimental testing is shown in Figure 5 attached to the tip of the arm. It shows the telescopic element (associated with motion d_5) as well as the needle (associated with motion d_6) at an extended position. The needle grip is secured on a slider block that moves along a linear guide. The needle tip passes through a disposable guide at the bottom edge of the end–effector. For the localization of the needle prior to body or phantom puncture, a pair of parallel cylindrical tubes, filled with a gadolinium chelate solution of 0.01 mM (Magnevist, Bayer Shering Pharma, Berlin, Germany), is symmetrically placed on either side of the needle guide. These will appear in the MR images as two bright lines facilitating the targeting procedure [16].

IV. EXPERIMENTAL TESTING

Preliminary testing of the prototype manipulator constructed was carried out to assess its magnetic compatibility. Testing was performed inside two cylindrical closed–type scanners with 1.5T and 3T static magnetic fields, respectively (Philips, Medical Systems, Best, The Netherlands). The modular system design allowed testing of the individual components of the system for magnetic field–related translational attraction and torque. As expected, all parts were found to have no magnetic field interactions in association with exposure to the used MR systems. Finally, the system's presence does not introduce any notable imaging artifacts (end–effector tools were not tested).

For an initial evaluation of its tip positioning accuracy the system was placed on a table over a grid paper serving as a reference for position measurements. Its was then manually adjusted to different configurations (N=40) selected to span its workspace by manually setting the joint positions. The

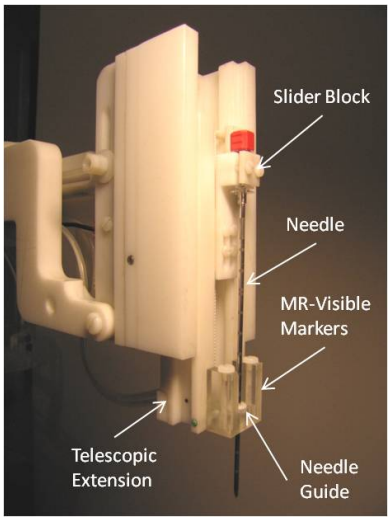

Fig. 5. The end–effector attached at the tip of the arm holding a general–purpose needle.

cartesian tip positions calculated using forward kinematics were compared with the measured ones. The average distance between them was 3.8 mm (with standard deviation 0.8 mm). Further testing involved MR–visible phantoms to assess the manipulator's effectiveness in performing needle targeting tasks as required in various minimally invasive interventions (e.g., biopsies, aspirations and local drug deliveries). Testing of the system has demonstrated that a significant advantage of the manipulation system is its intuitive kinematic structure. This allowed the operating physician to quickly become accustomed with its operation following minimal training. The arc–shaped base was found to be sufficiently stiff so that compliance does not compromise the required tip positioning accuracy. Phantom experiments were carried out to evaluate the image–guided target acquisition capability of the system. The phantom consisted of a plastic container filled with animal fat (butter) into which five spherical objects (3, 5, 10, 15, 20 mm in diameter plasticine balls) were immersed to represent targets. Repeated targeting attempts were carried out for each individual target along five different access paths. The smallest–size target with 100% successful acquisitions was the 5 mm in diameter.

A preoperative planning procedure enabled by a suitable software tool [16] involves (a) registration of the scanner's coordinate reference system to that of the robot's through the acquisition of scout images, (b) acquisition of a stack of parallel images of the anatomy under investigation, and (c) delineation by the user of the target and critical regions–of–interest (ROIs) on each acquired image. The software then proceeds with an inverse kinematics solution of the manipulator joints yielding the set of possible insertion vectors through permissible access paths. After examining the available options, the physician selects the most appropriate solution taking into account different criteria (required depth of insertion, proximity of needle path to critical ROIs, etc).

The phantom used for the results presented herein consists

of a plastic container filled with animal fat (butter) in which a grape of about 1 cm in diameter was immersed to represent the target. To mimic impenetrable structures (e.g., bones) and critical organs, additional structures were embedded into the fat matrix. In particular, a bony structure was represented by a group of vitamin capsules retained inside a small plastic container which was placed a few centimeters above the target. To represent sensitive structures, which also have to be avoided by the needle while moving towards the target, a sealed plastic container filled with an aqueous solution (0.01 mM) of a paramagnetic contrast agent (Magnevist, Bayer Shering Pharma, Berlin, Germany) was placed at the side of the target. Imaging was performed in a cylindrical 1.5T scanner with a bore diameter of 60 cm (NT–Intera, Philips, Medical Systems, Best, The Netherlands). The built–in quadrature RF body coil was used for both excitation and signal reception. T1–weighted gradient echo images (4.6 and 7.7 ms echo and repetition times, respectively) were acquired for localization purposes and fluoroscopic imaging of the target acquisition procedure was implemented. A MR–compatible 20G needle was used (MRI Chiba Needle, Somatex Medical Technologies, Teltow, Germany).

Figure 6a shows a software–reconstructed 3D representation of the phantom lying on the table top at the scanner's isocenter vicinity. The defined target ROI (green) and the critical ROIs (red) can be seen within its volume. A line representation of the robot position corresponding to the selected needle path is also shown. The planning software provides the user with the corresponding values of the joint variables required for the selected positioning of the end–effector with the needle aligned with the specified target ROI. Using these values the manipulator is manually adjusted to this position (using the ruler/protractor marks related to each linear/rotational joint) and image acquisition is used to confirm that the needle is correctly pointing towards the target. If required small manual adjustments are carried out prior to commencing the needle insertion, which can be monitored under real–time imaging. Figure 6(b,c) show the needle en route towards the target and after it has successfully acquired the target, respectively. The needle is actually visualized in the image through the magnetic susceptibility artifact that generates. Successful target acquisition was accomplished in successive trials using the inverse kinematics solution depicted in Figure 6a as well as alternative access paths.

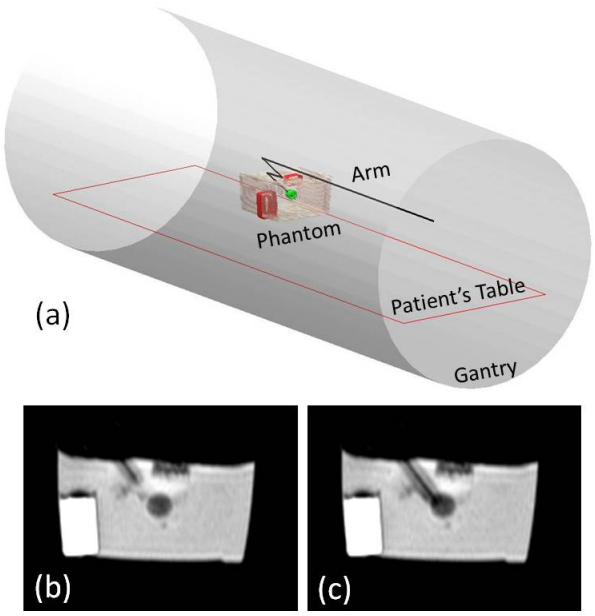

Fig. 6. Experimental phantom study on image–guided targeting using the prototype MR–compatible manipulation system. (a) Output of the preoperative stereotactic planning tool for the acquisition of a selected target ROI (green structure) while avoiding defined critical ROIs (red structures). (b) Intraoperative MR image showing the needle en route towards the target. (c) MR image showing the needle while acquiring the target.

V. DISCUSSION

The herein presented prototype system demonstrated that manual actuation is a practical option for robotic manipulators performing MR–guided interventions. Compared to devices with computer–controlled actuators a manual device presents various advantages including simplicity and lower cost. Also, it is anticipated that obtaining the required permissions from regulatory agencies prior to clinical use will be significantly simplified due to the absence of active and automated components. Admittedly, a main limitation of the manual actuation approach is that the system may not take full advantage of computer–control capabilities (e.g., automatic execution of a preoperative plan). From a physician's perspective, performing an intervention using the manual system will in fact be perceived as an extension to the familiar manual practices in interventional radiology.

An important feature of the manual actuation option is that the operator can feel on the control handles the forces applied on the end–effector and the penetrating needle. A more realistic sensation of the applied forces/torques on the end–effector is available to the operator when direct transmissions are used (e.g., no leverage or gear reductions are involved). Also, minimization of friction and flexibility in the transmission mechanisms constitutes this haptic–like sensation even more realistic and accurate. Achievement of such passive haptic feedback can be considered as an advantage of the current design, or any other similar manually–actuated robotic device. Otherwise, the implementation of haptic feedback on an MR–compatible computer–controlled and actuated system would require the incorporation of specialized MR–compatible force sensors on the end–effector.

In our system the arm is mounted on an arc–shaped structure. Several different mounting options exist with the most commonly used being to mount the robotic device on the scanner's table (e.g., [8], [15]), or on a separate supporting structure (e.g., [9], [17]). A more distinct approach was used in [18] where the robotic device was patient–mounted. Various criteria need to be considered when selecting the most appropriate mounting option which will also depend on the clinical applications and the scanner type that will be used. Transportability and ease of installation are among the important factors. It is unlikely that the expected return–

on–investment will justify that an MR scanning facility will be dedicated to robotically–assisted interventions. Therefore, permanently installed mounting fixtures (on the floor, ceiling or walls) are not expected in a scanner room as for example in the case of robots operating in a manufacturing facility. The choice of an arc–shaped mounting structure, that also allows motion of the system along its curve, serves well a general–purpose device such as the one developed in this work. Also, the used mounting structure does not seriously obstruct the access to the patient. Structural stiffness and mounting position stability are good as suggested by the high repeatability achieved with regard to target acquisition in successive trials during experimental testing.

For any system whose operation involves a synergy between humans and equipment, consideration of human factors plays an important role in the system's design. In general, the discipline of human factors provides a framework for designing more ergonomic, functional, efficient and safer devices. Human factors play a significant role in the high–risk operations performed with healthcare systems [19]. Several relevant provisions were incorporated in the design of the presented system. First, its rather intuitive kinematics structure allows the operator to focus on the actual interventional task rather than being preoccupied with the operation of the device. For example, prior to maneuvering the end–effector the operator does not have to mentally solve the inverse kinematics of the manipulator. Second, the control of the system is rather intuitive since it is directionally compatible with the movement of the end–effector. Third, the operator can control the specific system from an ergonomically comfortable position while standing at the side of the scanner's bed and having direct view of the patient and the end–effector. From that position the physician can also view on a screen, placed by the scanner, the pre– or intra–operative acquired images as well as the output of the computer–assisted planning software. Fourth, regarding the controls apart from being reachable from the operator's normal working position, tactile coding was considered, i.e., making the controls identifiable by touch. The importance of this provision is apparent in the case of an image–guided procedure where the physician's attention is constantly focused on the intraprocedural images while manipulating surgical instruments.

Current and future work focuses on further developments of the preoperative planning tool and the manipulator itself. One area is to endow the software with the capability of evaluating all feasible target–acquisition solutions and selecting the optimal one. Another area is the design of specialized end–effectors which will expand the applications field. An important direction that is currently examined involves the installation of appropriate position sensors on the joints from which the position and orientation of the end–effector can be deduced (using the forward kinematics solution). This will allow integration of the system with the MR scanner in order to automatically update the imaging planes while the operator free–hand maneuvers the end–effector so that the interventional tool is automatically tracked [20].

REFERENCES

[1] C. R. Weiss, S. G. Nour, and J. S. Lewin, "MR-guided biopsy: a review of current techniques and applications," *Journal of Magnetic Resonance Imaging*, vol. 27, no. 2, pp. 311–325, 2008.

[2] A. Arepally, "Targeted drug delivery under MRI guidance," *Journal of Magnetic Resonance Imaging*, vol. 27, no. 2, pp. 292–298, 2008.

[3] A. Patriciu, D. Petrisor, M. Muntener, M. S. D. Mazilu D, and D. Stoianovici, "Automatic brachytherapy seed placement under MRI guidance," *IEEE Trans. on Biomedical Engineering*, vol. 54, no. 8, pp. 1499–1506, 2007.

[4] P. R. Morrison, S. G. Silverman, K. Tuncali, and S. Tatli, "MRI–guided cryotherapy," *Journal of Magnetic Resonance Imaging*, vol. 27, no. 2, pp. 410–420, 2008.

[5] N. V. Tsekos, A. Khanicheh, E. Christoforou, and C. Mavroidis, "Magnetic resonance–compatible robotic and mechatronics systems for image–guided interventions and rehabilitation: a review study," *Annual Review of Biomedical Engineering*, vol. 9, pp. 351–387, 2007.

[6] G. Schaefers, "Testing MR safety and compatibility," *IEEE Engineering in Mecicine and Biology Magazine*, vol. 27, no. 3, pp. 23–27, May/June 2008.

[7] K. Masamune, E. Kobayashi, Y. Masutani, M. Suzuki, T. Dohi, H. Iseki, and K. Takakura, "Development of an MRI–compatible needle insertion manipulator for stereotactic neurosurgery," *Journal of Image Guided Surgery*, vol. 1, no. 4, pp. 242–248, 1995.

[8] A. Melzer, B. Gutmann, T. Remmele, R. Wolf, A. Lukoscheck, M. Bock, H. Bardenheuer, and H. Fischer, "INNOMOTION for percutaneous image–guided interventions," *IEEE Engineering in Mecicine and Biology Magazine*, vol. 27, no. 3, pp. 66–73, May/June 2008.

[9] N. V. Tsekos, A. Özcan, and E. Christoforou, "A prototype manipulator for MR–guided interventions inside standard cylindrical MRI scanners," *ASME Journal of Biomechanical Engineering*, vol. 127, pp. 972–980, November 2005.

[10] G. R. Sutherland, I. Latour, and A. D. Greer, "Integrating an image–guided robot with intraoperative MRI: A review of the design and construction of neuroArm," *IEEE Engineering in Mecicine and Biology Magazine*, vol. 27, no. 3, pp. 59–65, May/June 2008.

[11] S. G. Hushek, A. J. Martin, M. Steckner, E. Bosak, J. Debbins, and W. Kucharzyk, "MR systems for MRI–guided interventions," *Journal of Magnetic Resonance Imaging*, vol. 27, no. 2, pp. 253–266, 2008.

[12] R. Gassert, D. Chapuis, H. Bleuler, and E. Burdet, "Sensors for applications in magnetic resonance environments," *IEEE/ASME Trans. on Mechatronics*, vol. 13, no. 3, pp. 335–344, June 2008.

[13] C. Keroglou, I. Seimenis, N. V. Tsekos, C. Pitris, E. Eracleous, and E. G. Christoforou, "Consideration of geometric constraints regarding MR–compatible interventional robotic devices," in *3rd IEEE/RAS-EMBS International Conference on Biomedical Robotics and Biomechatronics*, Tokyo, Japan, Tokyo 26–29 2010, pp. 355–360.

[14] M. Moche, D. Zajonz, T. Kahn, and H. Busse, "MRI–guided procedures in various regions of the body using a robotic assistance system in a closed–bore scanner: preliminary clinical experience and limitations," *J Magn Reson Imaging*, vol. 31, no. 4, pp. 964–974, 2010.

[15] D. Stoianovici, K. Cleary, A. Patriciu, D. Mazilu, A. Stanimir, N. Craciunoiu, V. Watson, and L. Kavoussi, "AcuBot: a robot for radiological interventions," *IEEE Trans. on Robotics and Automation*, vol. 19, no. 5, pp. 927–930, October 2003.

[16] I. Seimenis, N. V. Tsekos, C. Keroglou, E. Eracleous, C. Pitris, and E. G. Christoforou, "An approach for preoperative planning and performance of MR-guided interventions demonstrated with a manual manipulator in a 1.5T MRI scanner," *Cardiovasc Intervent Radiol*, vol. 35, no. 2, pp. 359–367, April 2012.

[17] K. Chinzei, N. Hata, A. Jolesz, and R. Kikinis, "MR compatible surgical assist robot: System integration and preliminary feasibility study," in *Proc. of Medical Image Computing and Computer–Assisted Intervention*, Pittsburgh, PA, October 11–14 2000, pp. 921–930.

[18] I. Bricault, N. Zemiti, E. Jouniaux, C. Fouard, E. Taillant, F. Dorandeu, and P. Cinquin, "A light puncture robot for CT and MRI interventions," *IEEE Engineering in Medicine and Biology Magazine*, vol. 27, no. 3, pp. 42–50, May–June 2008.

[19] R. L. Helmreich and A. C. Merritt, *Culture at Work in Aviation and Medicine: National, Organizational and Professional Influences*, 2nd ed. Ashgate, 2001.

[20] E. Christoforou, E. Akbudak, A. Ozcan, M. Karanikolas, and N. V. Tsekos, "Performance of interventions with manipulator-driven real-time MR-guidance: Implementation and initial in vitro tests," *Magnetic Resonance Imaging*, vol. 25, no. 1, pp. 69–77, 2007.